Ultrasonics Sonochemistry 73 (2021) 105543

Contents lists available at ScienceDirect

Ultrasonics Sonochemistry

journal homepage: www.elsevier.com/locate/ultson

Disinfection characteristics of an advanced rotational hydrodynamic cavitation reactor in pilot scale

Xun Sun [a,b], Zhengquan Wang [a,b], Xiaoxu Xuan [a,b,*], Li Ji [a,b], Xuewen Li [c], Yang Tao [d], Grzegorz Boczkaj [e], Shan Zhao [f], Joon Yong Yoon [g], Songying Chen [a,b,*]

[a] Key Laboratory of High Efficiency and Clean Mechanical Manufacture, Ministry of Education, School of Mechanical Engineering, Shandong University, Jinan 250061, China
[b] National Demonstration Center for Experimental Mechanical Engineering Education, Shandong University, Jinan 250061, China
[c] School of Public Health, Shandong University, Jinan 250061, China
[d] College of Food Science and Technology, Nanjing Agricultural University, Nanjing 210095, China
[e] Department of Process Engineering and Chemical Technology, Faculty of Chemistry, Gdańsk University of Technology, Gdańsk 80-233, Poland
[f] Shandong Key Laboratory of Water Pollution Control and Resource Reuse, School of Environmental Science and Engineering, Shandong University, Qingdao 266237, China
[g] Department of Mechanical Engineering, Hanyang University, Ansan 15588, Republic of Korea

ARTICLE INFO

Keywords:
Water disinfection
Sonochemistry
Hydrodynamic cavitation
E. coli
Disinfection mechanism

ABSTRACT

Hydrodynamic cavitation is a promising technique for water disinfection. In the present paper, the disinfection characteristics of an advanced hydrodynamic cavitation reactor (ARHCR) in pilot scale were studied. The effects of various flow rates (1.4–2.6 m^3/h) and rotational speeds (2600–4200 rpm) on the removal of *Escherichia coli* (*E. coli*) were revealed and analyzed. The variation regularities of the log reduction and reaction rate constant at various cavitation numbers were established. A disinfection rate of 100% was achieved in only 4 min for 15 L of simulated effluent under 4200 rpm and 1.4 m^3/h, with energy efficiency at 0.0499 kWh/L. A comprehensive comparison with previously introduced HCRs demonstrates the superior performance of the presented ARHCR system. The morphological changes in *E. coli* were studied by scanning electron microscopy. The results indicate that the ARHCR can lead to serious cleavage and surface damages to *E. coli*, which cannot be obtained by conventional HCRs. Finally, a possible damage mechanism of the ARHCR, including both the hydrodynamical and sonochemical effects, was proposed. The findings of the present study can provide strong support to the fundamental understanding and applications of ARHCRs for water disinfection.

1. Introduction

Water scarcity has been a serious worldwide problem, driven by a combination of population growth, industrialization, environmental pollution, and inappropriate use and reutilization [1,2]. Nowadays, over two billion people are suffering from high water stress worldwide [3]. In accordance with the data from the Ministry of Environmental Protection of China, over 280 million Chinese are facing the potential safety issue of drinking water. Therefore, it is becoming increasingly important to recycle wastewater (WW) and assure the quality of drinking water sources [4]. Within the WW treatment process, disinfection is a necessary step to eliminate pathogenic microorganisms that are responsible for waterborne diseases.

To overcome the shortcomings of conventional chemical and physical methods, researchers recently proposed several new technologies, such as UV-LEDs [5], copper-silver ionization [6], electrochemistry [7], photocatalysis [8], solar [9], nanocomposite [10], and cavitation [11]. Cavitation has been widely considered as a promising, environmental-friendly disinfection technique [12]. Cavitation phenomenon is a rapid phase transition process, including bubble formation, growth, and collapse, in liquid in a considerably short period [13]. The huge energy release, in the form of mechanical, thermal, and chemical effects, during

* Corresponding authors at: Key Laboratory of High Efficiency and Clean Mechanical Manufacture, Ministry of Education, School of Mechanical Engineering, Shandong University, 17923, Jingshi Road, Jinan, Shandong Province, 250061, China.
E-mail addresses: xunsun@sdu.edu.cn (X. Sun), 202034380@mail.sdu.edu.cn (Z. Wang), xiaoxuxuan@sdu.edu.cn (X. Xuan), liji@sdu.edu.cn (L. Ji), lxw@sdu.edu.cn (X. Li), yang.tao@njau.edu.cn (Y. Tao), grzegorz.boczkaj@pg.edu.pl (G. Boczkaj), szhao@sdu.edu.cn (S. Zhao), joyoon@hanyang.ac.kr (J.Y. Yoon), chensy66@sdu.edu.cn (S. Chen).

https://doi.org/10.1016/j.ultsonch.2021.105543
Received 1 February 2021; Received in revised form 12 March 2021; Accepted 23 March 2021
Available online 3 April 2021

bubble collapse is highly destructive to microorganisms. Moreover, as a result of the created extreme conditions, cavitation can be effectively combined with various physical and chemical means, e.g., oxidants [14], UV [15], and plasma [16].

Acoustic cavitation (AC) is a highly effective tool to inactivate microorganisms in small scales [17], however, scaling it up for industrial applications can result in unrealistic operational and equipment costs [18]. On the contrary, hydrodynamic cavitation (HC), with the similar mechanism with AC, has been widely considered as an alternative technology to AC for large scales, as the advantages of good scalability, simple design, and low price [19]. Because HC phenomenon is induced by hydrodynamic cavitation reactors (HCRs), thus, HCR performance determines the disinfection effectiveness and cost [20]. In the past, various types of HCRs have been utilized to inactivate bacteria, yeasts, cyanobacteria, microalgae, and viruses, as demonstrated in Fig. 1 and Supplementary Table S1. In accordance with cavitation generation mechanism, HCR can be classified as non-rotational (based on constriction effect) and rotational (based on shear effect). Non-rotational HCRs (such as orifices or Venturis) and simple rotational HCRs are widely studied in various applications, as their high commercialization, simple design, and ease of operation. Recently, few advanced rotational HCRs (ARHCRs) with rotor-stator assembly have shown superior performance in disinfection [21], as well as organic degradation [22], food processing [23], delignification [24], waste-activated sludge (WAS) treatment [25], refining of cellulose pulp [26], and biodiesel synthesis [27], etc., compared with that of conventional HCRs.

Nevertheless, few researchers have focused on disinfection by ARHCRs [21,28-32]. To the best of our knowledge, no researcher has investigated the disinfection effectiveness of ARHCRs under a wide range of operating conditions (i.e., flow rate and rotational speed) in the past. No work has established the relationship between the cavitation number and effectiveness. Moreover, the damage mechanism of ARHCRs has never been involved. The above issues have been greatly hindering the theoretical development of ARHCRs, as well as the commercialization progress of HC disinfection technology.

To this end, the present work investigated the disinfection characteristics of a representative, pilot-scale ARHCR which was studied in our previous studies [33-35]. The effects of various flow rates and rotational speeds on removing *Escherichia coli* (*E. coli*) in simulated effluents were evaluated with explanations of possible mechanisms. Then, a comprehensive comparison between the ARHCR and other previous HCRs was conducted with the emphasis on disinfection rate, treatment rate, and energy efficiency. Finally, the possible damage mechanism was proposed in accordance with the scanning electron microscopy (SEM) results.

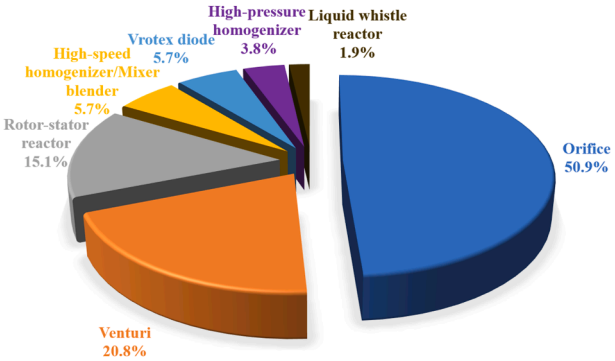

Fig. 1. Various HCRs utilized in the previous HC disinfection and cell disruption studies in the past 30 years (sector area stands for the proportion).

2. Materials and methods

2.1. Experiment setup

The 22-kW-class ARHCR consists of a front cover, a side cover, a rear cover, and a rotor, as demonstrated in Fig. 2. To artificially generate cavitation bubbles, numerous cavitation generation units (CGUs) were processed on the rotor surfaces and the inner surfaces of the covers. Fig. 3 illustrates a schematic of an open-loop ARHCR experiment system with a treatment capacity of 100 L. By uncertainty analysis, the standard uncertainties of the obtained quantities (e.g., temperature, flow rate, pressure, shaft power (P_t), heat generation rate (HGR, $\dot{H}$), and thermal efficiency (TE, η_t)) in the present study only accounted for less than 0.5% of the maximum values, this indicates that the measured and calculated quantities are reliable, as presented in Supplementary Table S2. Specifics of the ARHCR structure, experimental setups, and definitions of HGR and TE can be found in our previous work [33].

2.2. Experimental procedure

To investigate the disinfection characteristics, the effects of two important operational variables, namely, rotational speed (2600, 3000, 3400, 3800, and 4200 rpm) and flow rate (1.4, 2.0, and 2.6 m^3/h) were evaluated. In total, 15 cases were conducted, as shown in Supplementary Table S3. In each case, 15 L of distilled water, which contained *E. coli* with an initial concentration of $\sim 10^6$ CFU/ml, was repeatedly treated by the ARHCR for 10 min. The initial temperature for each case was set as 27–29 °C. During each case, 100 ml samples were collected at 0, 2, 4, 6, 8, and 10 min. The tank, inlet, and outlet water temperatures, outlet flow rate, and shaft power were recorded with a data acquisition frequency of 1.2 time/s. The detailed information on microorganism and corresponding analytical methods can be found in our previous study [33].

2.3. Microorganisms morphology

To confirm the destruction effect of the ARHCR, the morphological changes of *E. coli* cells before and after treatment at a rotational speed of 3800 rpm and a flow rate of 2.0 m^3/h were observed by a scanning electron microscope (SU-8010, Hitachi, Japan). The samples were washed three times with 0.1 M phosphate buffer (pH 7.0) for 15 min, fixed with 1% osmic acid solution for 2 h, and then washed three times with 0.1 M phosphate buffer (pH 7.0) for 15 min. Samples were dehydrated via successive passages through 30, 50, 70, 80, 90, 95, and 100% ethanol (15 min per step).

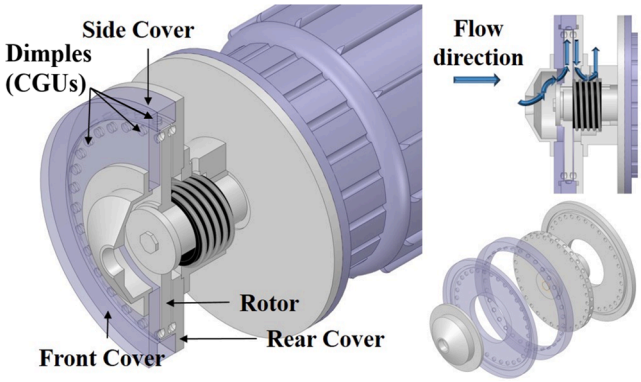

Fig. 2. Schematic diagram of the ARHCR.

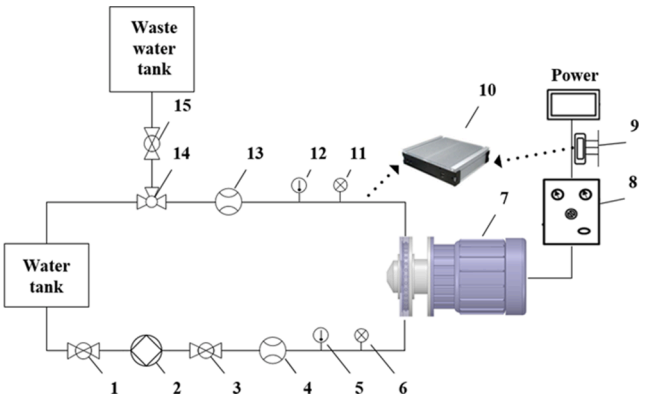

Fig. 3. Schematic diagram of the ARHCR experimental setup. (PID represents proportional integral differential, ARHCR represents advanced rotational hydrodynamic cavitation reactor, and IPC represents industrial personal computer). 1, 15-ball valves; 2-jet pump; 3-PID control valve; 4, 13-electromagnetic flowmeters; 5, 12-temperature sensors; 6, 11-pressure sensors; 7-ARHCR and electrical motor; 8-control cabinet and frequency transformer; 9-power meter; 10-IPC and 485 hub; 14-T-port valve.

3. Results and discussion

3.1. Effect of operational conditions

The thermal performance of the ARHCR, which is considered as an intuitive factor characterizing cavitation intensity [36], was evaluated combining with the disinfection results in the present study. Table 1 shows the variations in the thermal and disinfection characteristics and energy consumption of the ARHCR at various rotational speeds and flow rates. In the case of 4200 rpm and 2.6 m^3/h, because the water started to boil during the treatment and cannot be pumped to the ARHCR, therefore, the corresponding disinfection result is not included. In addition, since water temperature gradually increased from 27 to 29 °C during the treatment, the final temperature, T_{final}, in Table 1 indicates the water temperature at 10 min. The detailed concentration and water temperature variations in each case can be found in Supplementary Table S4.

3.1.1. Effect of rotational speed

For the thermal characteristics of the ARHCR, taking the case of 1.4 m^3/h as an example, an increase in the rotational speed from 2600 to 4200 rpm caused the increase in the HGR from 3.49 to 11.22 MJ/h, while the TE almost remained the same (from 78.94% to 78.99%), as shown in Table 1. Our previous studies showed the same variation trend, for example, Sun, et al. [36] reported that increasing the rotational speed of an ARHCR from 2700 to 3600 rpm led to approximately two times HGR for each pump pressure. Fig. 4 presents the variations in the *E. coli* concentration at various rotational speeds (from 2600 to 4200 rpm) and the same flow rate (1.4 m^3/h). The effect of rotational speed on disinfection was significant. Even though only 96.39% of *E. coli* was eliminated in 10 min at 2600 rpm (corresponding to 1.44 log CFU/mL reduction), once the rotational speed was increased greater than 2600 rpm, 100% elimination rates were easily achieved in 10 min. In the case of 4200 rpm, the treatment time was reduced to even 4 min. On the whole, an increase in the rotational speed from 2600 to 4200 rpm increased the reaction rate constant from 5.48×10^{-3} to 63.03×10^{-3}/s. This trend was also confirmed by Milly, et al. [30], who found that when the rotational speed of the ARHCR was increased from 3000 to 3600 rpm, the log reduction of *Bacillus coagulans* spores in tomato juice was significantly enhanced from 0.88 ± 0.10 to 3.10 ± 0.21 for the same exit temperature. In addition, the benefit of high rotational speeds was also confirmed in other applications, e.g., wastewater treatment [15,22,37,38], delignification [24], WAS treatment [39,40], refining of cellulose pulp [26], removal of cyanobacteria [28], and biodiesel production [41].

In accordance with our previous work regarding computational fluid dynamics (CFD) [34], the rotational speed basically determines the cavitation intensity of ARHCRs. This is because high rotational speeds cause large separation regions on the downstream side of the CGUs and strong vortexes inside the CGUs, which can result in large sheet cavitation and vortex cavitation regions. Moreover, because cavitation is compulsorily generated and crushed by the periodic interaction between the static and moving CGUs, higher rotational speeds also result in higher generation and collapse frequencies. Because of the above two reasons, ARHCRs operating at high rotational speeds can achieve satisfactory treatment effectiveness.

On the other hand, as the pressure and friction resistances of the fluids and the friction loss of the transmission system rapidly increase with increasing rotational speed, higher required electrical inputs of the motor are accompanied. For instance, the required shaft power was increased from 4.42 to 14.21 kW by raising the rotational speed from 2600 to 4200 rpm at 1.4 m^3/h. Therefore, to maximize the disinfection effectiveness and economic efficiency, it is vital to specify a proper rotational speed. For example, for the same treatment time (10 min) and flow rate (1.4 m^3/h), the disinfection rates at 3000 and 3400 rpm were the same (100%), however, the energy consumptions were 1.028 and 1.388 kWh, respectively. In addition, cavitation and impurities can

Table 1
Thermal and disinfection performance of the ARHCR at various operational conditions.

ω (rpm)	Q_{in} (m^3/h)	$\dot{H}$ (MJ/h)	P_t(kW)	η_t(%)	P_{out}(kPa)	T_{final}(°C)	$C_{initial}$ (CFU/ml)	C_{final} (CFU/ml)	Log reduction	Reaction rate constant ($\times 10^{-3}$/s)	Energyconsumption (kWh)
2600	1.4	3.49	4.42	78.94	17.86	45.1	6.43 ± 0.08 [a]	4.99 ± 0.09	1.44	5.48	0.737[b]
	2	3.63	4.50	80.57	36.85	48.8	7.20 ± 0.05	6.08 ± 0.09	1.12	4.30	0.750
	2.6	3.72	4.45	83.62	61.44	48.4	6.39 ± 0.09	6.03 ± 0.07	0.36	1.38	0.742
3000	1.4	4.77	6.17	77.38	17.74	54.9	4.84 ± 0.21	0 (10 min, 54.9 °C)	4.84	17.88	1.028
	2	5.05	6.26	80.68	36.58	57.0	7.30 ± 0.01	5.97 ± 0.03	1.33	5.10	1.043
	2.6	5.14	6.22	82.64	61.86	60.5	6.50 ± 0.03	4.46 ± 0.08	2.04	7.83	1.037
3400	1.4	6.56	8.33	78.79	17.93	70.8	6.64 ± 0.03	0 (10 min, 70.8 °C)	6.64	25.48	1.388
	2	6.87	8.55	80.34	36.51	66.7	6.54 ± 0.01	4.35 ± 0.05	2.19	8.40	1.425
	2.6	7.20	8.86	81.31	61.67	72.2	7.55 ± 0.01	4.62 ± 0.02	2.93	11.24	1.477
3800	1.4	8.27	10.31	80.16	18.02	75.2	6.59 ± 0.03	0 (8 min, 65.9 °C)	6.59	31.61	1.375
	2	8.85	11.08	79.88	36.25	77.4	6.42 ± 0.12	0 (10 min, 77.4 °C)	6.42	24.63	1.847
	2.6	8.99	11.06	81.30	61.57	83.0	7.49 ± 0.01	4.97 ± 0.04	2.52	9.67	1.843
4200	1.4	11.22	14.21	78.99	17.83	88.4	6.57 ± 0.04	0 (4 min, 53.3 °C)	6.57	63.03	0.748
	2	11.44	14.14	80.88	36.73	89.2	6.01 ± 0.03	0 (10 min, 89.2 °C)	6.01	23.06	2.357
	2.6	11.26	14.05	80.14	61.51	–	–	–	–	–	–

[a] The value is expressed as mean ± standard deviation (n = 3).
[b] The value is calculated in terms of the shaft power and treatment duration.

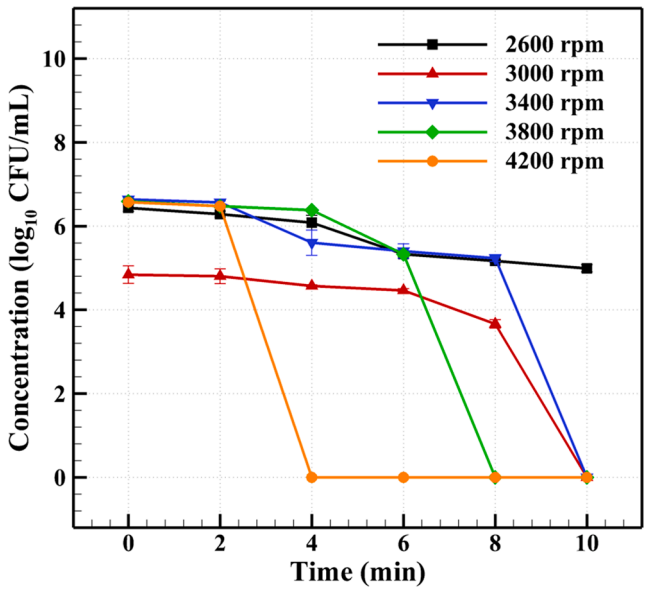

Fig. 4. Effect of rotational speed on the removal of *E. coli* at a flow rate of 1.4 m^3/h.

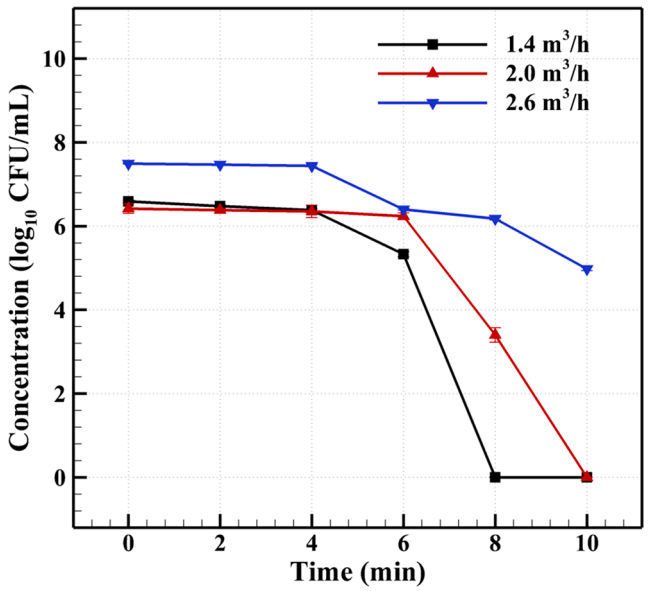

Fig. 5. Effect of flow rate on the removal of *E. coli* at a rotational speed of 3800 rpm.

cause serious erosion damage at high rotational speeds [42], which has to be considered in real applications.

3.1.2. Effect of flow rate

Our previous study [32] indicates that the flow rate is a positive factor influencing the disinfection effectiveness of the ARHCR in batch mode: disinfection rates at 35.45% and 100% for *E. coli* were obtained at the flow rates of 8 and 11 L/min under the same duration (12 min) and rotational speed (3600 rpm), respectively. However, the result of the present work shows an opposite trend, as shown in Fig. 5 which indicates the variations in the *E. coli* concentration at various flow rates (from 1.4 to 2.6 m^3/h) and the same rotational speed (3800 rpm). The ARHCR achieved log reductions of 6.59 (corresponding to a disinfection rate of 100%) and 6.42 (100%) in 8 min and 10 min at 1.4 and 2 m^3/h, respectively. While when the flow rate was increased to 2.6 m^3/h, the log reduction was reduced to 2.52 (99.70%) in 10 min. This trend is also confirmed by Šarc, et al. [21], who found that the log reduction for *E. coli* achieved by an ARHCR was increased from 0.24 to 3.3 by decreasing the flow rate from 1.8 to 0.2 L/min with 200 times less electrical consumption under the same rotational speed. This was attributed to the super-HC condition created by the considerably low flow rate. Moreover, we recently found that when the flow rate was reduced from 5.5 to 4.2 L/min at the same rotational speed (3600 rpm) and final treatment temperature (70 ℃) of the ARHCR in continuous mode, the log reduction for *E. coli* was enhanced from 2.20 ± 0.07 (99.87%) to 5.76 ± 0.07 (100%). This trend can be explained as follows: when the same rotational speed is constant, the cavitation intensity produced by the ARHCR is "concentrated" at lower flow rates, leading to greater destruction effects, and vice versa. The detailed mechanism is needed to be further investigated by CFD.

To visually present the effect of rotational speed and flow rate, Fig. 6 presents the variations in the log reduction and reaction rate constant at various C_v (its definition can be found in Sun, et al. [33]). In general, C_v less than 1 indicates that fluid devices are operated under cavitation conditions [43]. The maximum C_v in the present study is 0.289, signifying the ARHCR was operated under severe cavitation conditions in all cases. Overall, the variation trends of the log reduction and reaction rate constant were considerably similar. A decrease in the C_v from 0.289 to 0.087 contributed to the rapid increases in both the log reduction (from 0.36 to 6.57) and reaction rate constant (from 1.38×10^{-3} to 63.03×10^{-3} /s). Operating the ARHCR at low cavitation numbers can significantly enhance the disinfection effectiveness. This variation trend is identical to that of disinfection by orifice plates, as summarized in Burzio, et al. [44]'s work, while the reaction rate constant of the ARHCR was considerably higher than that of orifices.

3.1.3. Effect of final treatment temperature

Temperature can affect various physical properties of water, e.g., vapor pressure, surface tension, viscosity, and dissolved gas content [45]. As a result, the formation, radius, and lifetime of the cavitation bubble and cavitation intensity can be changed at various temperatures. In addition, temperature also influences chemical reaction rates. Therefore, treatment temperature is important for HC treatment effectiveness, as confirmed in various applications, such as WAS treatment [46], degradation of organic matter [47], biodiesel production [48], and disinfection [49]. For the disinfection by ARHCRs in continuous mode, the final treatment temperature is a vital factor. For example, we found that log reductions for *E. coli*, *Staphylococcus aureus*, and *Bacillus cereus* were improved from 3.34 ± 0.01 to 5.73, 1.27 ± 0.08 to 5.53, and 1.89

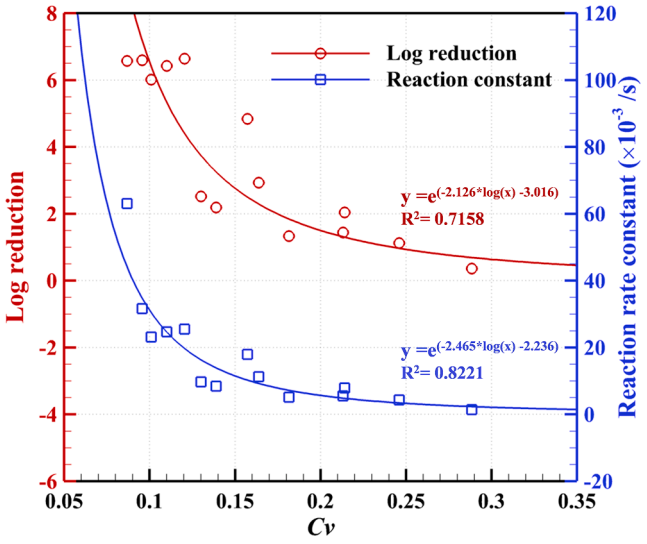

Fig. 6. Effect of cavitation number on the log reduction and reaction constant of the disinfection process.

± 0.16 to 2.99 ± 0.08, respectively, by increasing the final temperature from 60 to 70 ℃ [35]. This trend was also reported by Milly, et al. [30].

In our previous study [32], we supposed that *E. coli* can be completely eliminated no matter how long the treatment lasts if the temperature reaches a certain value when the ARHCR is operated in batch mode. Nevertheless, the results in the present study overturned this. For instance, 100% of *E. coli* was eliminated (corresponding to a log reduction of 4.84) at 3000 rpm and 1.4 m^3/h with a final temperature at 56.6 ℃. When the final temperature was increased to 83 ℃ at 3800 rpm and 2.6 m^3/h, the ARHCR only achieved the disinfection rate at 99.70% (corresponding to a log reduction of 2.52) with the same duration. It can be concluded that the final temperature is not associated with the disinfection effectiveness of the ARHCR in batch mode for relatively small treatment capacity (15 L) and short treatment period (10 min). The effect of final temperature for pilot- or full-scale applications is needed to be further studied. Moreover, the thermal performance is not a universal index characterizing cavitation intensity induced by HCRs.

3.2. Performance evaluation

In order to comprehensively evaluate the disinfection performance, the disinfection rate, treatment rate, and energy efficiency of the ARHCR were compared with those of the HCR reported in the previous works regarding eliminating *E. coli*, as presented in Table 2. The treatment rate (L/min) is the ratio of the treatment volume (L) to treatment time (min) and the energy efficiency (kWh/L) is the product of the power (kW) and treatment time (h) per unit test volume.

Before 2010, the disinfection rate of conventional HCRs (such as Venturis or orifice plates) was relatively low, even they are combined with chemicals [50]. By continuous research and improvement, they are able to achieve satisfactory disinfection effects at a pilot scale. For instance, an orifice proposed by Dalfré Filho, et al. [54] obtained a disinfection rate at 100% with a treatment rate at 1.33 L/min and energy efficiency of 0.325 kWh/L, its performance is much higher than that of the early devices in the studies by Chand, et al. [50], Arrojo, et al. [51], and Mezule, et al. [52]. Recently, Prof. Ranade's group focuses on disinfection by utilizing vortex diode [55]: they found that 98.8% of *E. coli* can be removed with a considerably low energy consumption of 0.000525 kWh/L which is 618 times less than that of Dalfré Filho, et al. [54]'s device. Moreover, they also confirmed that cavitation behavior of the vortex diode can be enhanced by adding natural oils, e.g., eucalypts and clove oils with a small concentration of 0.1%, resulting in increased rates of disinfection (with the order of 2–4 folds) and shorter treatment duration [56]. However, it is difficult to completely remove pathogenic bacteria by the vortex diode.

On the other hand, few disinfection studies regarding ARHCRs have been published recently. The performance of laboratory-scale ARHCRs is relatively limited. Although the obtained values of disinfection effectiveness are relatively high, however, the treatment rate and energy efficiency are close or even lower to those of conventional HCRs, as found in Šarc, et al. [21]'s and Cerecedo, et al. [31]'s works. When ARHCRs are enlarged to pilot scales, they show great advantages in performance [32]. Compared with the laboratory-scale device utilized by Cerecedo, et al. [31], the present ARHCR achieved 116 times greater treatment rate and 51 times more economic efficiency, based on obtaining a disinfection rate at 100%. Moreover, the treatment rate was increased by 1.8 times than that of the orifice presented by Dalfré Filho, et al. [54], with 5.5 times more energy efficiency. Therefore, ARHCRs have great potential for industrial-scale disinfection or other process intensification applications.

In general, the performance of pilot-scale ARHCRs is far superior to that of conventional HCRs [38]. This is because that in ARHCRs the cavitation bubbles are compulsorily induced and destroyed by rotor motion and the rotational choke only occurs at a considerably high rotational speed, resulting in high cavitation generation efficiency [57]. While for conventional HCRs, choke cavitation can be easily formed by increasing the pressure difference between the upstream and downstream sides. Except for disinfection, ARHCRs also show overwhelming advantages in various applications. Taking WAS treatment as an example, due to limited cavitation intensity, conventional HCRs exhibited low disintegration degrees (DDs) of 7.7 to 31%, with substantial costs caused by high-power pumps [58-62]. Petkovšek, et al. [39] easily achieved a DD of approximately 57% by an ARHCR with only 20 passes for 100 L.

Nevertheless, because the comparison was based on the performance of previous HCRs with various operational conditions and structures in laboratory scale, more proper and comprehensive comparisons of effectiveness and cost (including equipment, operational, and maintenance costs) between conventional HCRs and ARHCRs at different scales are needed in future.

3.3. Disinfection mechanism

To study the cavitation damage effect on *E. coli*, the difference in cell morphology before and after the ARHCR treatment at 3800 rpm and 1.4 m^3/h was observed by utilizing SEM, as shown in Fig. 7. Fig. 7 (a) and

Table 2
Comprehensive performance comparison of the previous HCRs for inactivating *E. coli*.

Year	Study	Treatment method	**Disinfection rate (%)**	Test volume (L)	Treatment time (min)	**Treatment rate (L/min)**	Electricity consumption (kWh)	**Energy efficiency (kWh/L)**
Conventional HCRs								
2007	Chand, et al. [50]	Orifice + O_3	**72.88**	4	180	**0.022**	15.3 [a]	**3.825**
2008	Arrojo, et al. [51]	Orifice	**32.67**	60	120	**0.5**	18 [a]	**0.3**
		Venturi	**91.13**	60	120	**0.5**	18 [a]	**0.3**
2009	Mezule, et al. [52]	Milling cutter	**75**	2	3	**0.67**	0.098	**0.049**
2012	Loraine, et al. [53]	Venturi	**99.999**	1.8	120	**0.015**	0.935	**0.519**
2015	Dalfré Filho, et al. [54]	Orifice	**100**	40	30	**1.33**	12.99	**0.325**
2018	Šarc, et al. [21]	Venturi	**75.4**	4	120	**0.033**	2 [a]	**0.5**
2019	Jain, et al. [55]	Vortex diode	**98.8**	12	60	**0.2**	0.0063	**0.000525**
2020	Burzio, et al. [44]	Orifice	**99.4**	21	360	**0.0583**	3 [a]	**0.143**
Novel HCRs								
2018	Šarc, et al. [21]	ARHCR	**99.95**	2	150	**0.013**	0.7 [a]	**0.35**
2018	Cerecedo, et al. [31]	ARHCR	**100**	0.25	7.8	**0.032**	0.65	**2.6**
2018	Sun, et al. [32]	ARHCR	**100**	60	14	**4.3**	3.48	**0.058**
Present study		ARHCR	**100**	15	4	**3.75**	0.748	**0.0499**

[a] No information available on electricity consumption, but the required electric energy was calculated by the power rating.

(b) show the intact nature of rod-shaped *E. coli* with homogeneous and smooth surfaces before the treatment. After 10 min' treatment, the cell morphology was significantly changed (Fig. 7 (c)): A large number of cells agglomerated and their surfaces became creased. Fig. 7 (d) gives a detailed demonstration of the damage induced by the ARHCR. Cell membranes of most *E. coli* were ruptured as evident from the hole formation on the surfaces, resulting in loss of cytoplasm and leakage of cytoplasmic content. Moreover, some cells were even cut off from the middle.

In accordance with the above SEM results, it can be found that the damage behavior of the ARHCR was completely different from that of conventional HCRs. In general, Venturis and orifices can lead to severe surface damage to microorganisms, while the caused cell cleavage is considerably limited. This is discovered by Xie, et al. [63], who applied atomic force microscopy to qualitatively and quantitatively evaluate the morphological changes of *E. coli* induced by the viscous shear, collision, and HC (orifice) effects in water. They found that HC treatment significantly increased the surface roughness of *E. coli* from 0.63 ± 0.021 to 10.3 ± 2.11 nm (corresponding to the surface damage of 47 ± 3.65%), while the cell cleavage was limited: 2.01 ± 0.95%. In contrast, the shear and collision effects resulted in obvious cell cleavage of 20.65 ± 3.36% and 38.98 ± 4.16% and minor surface damages of 3.11 ± 1.24% and 2.87 ± 1.10%, respectively, which were opposite to the HC effect. In the present work, the ARHCR led to both severe cleavage and surface damages to *E. coli*, as shown in Fig. 7 (c) and (d), which demonstrates that the viscous shear, collision, and HC effects can be simultaneously acted on microorganisms during the ARHCR treatment.

The possible disinfection mechanism of the ARHCR can be divided into two categories: hydrodynamical and sonochemical, as demonstrated in Fig. 8. The hydrodynamical disinfection includes viscous shear and collision effects (Fig. 8 (a)). In the ARHCR, the fluid, which is driven by the rotor, flows into the CGUs and forms vortexes inside the CGUs. In addition, it also punches the downstream wall of the CGUs and generates separation regions. At high rotational speeds, both the dimension and intensity of the vortexes and separation regions are enormous, leading to considerably high local turbulent intensity and strong shear force. In addition, the fluid with high velocities (e.g., over 20 m/s at 3600 rpm [34]) can result in violent impacts on the CGU edges. Therefore, both the above effects can destroy *E. coli* by cleavage. Detailed information on the ARHCR flow field can be found in our previous work [34].

The sonochemical disinfection mechanism can be attributed to the synergy of mechanical, thermal, and chemical effects as cavitation bubbles collapse [4,12,57], as presented in Fig. 8 (b). The mechanical effect, which is induced by the violent shape change of the collapsing bubble, includes shock waves (with the average propagation velocity of 2000 m/s [64] and pressure as high as 7150 GPa [65]), microjets (with the maximum speed over 150 m/s [66], corresponding to over 200 MPa of water-hammer pressure [67]), and high shear stress (3.5 kPa [68]). This can cause generalized membrane rupture and loss of cytoplasm and periplasm [31]. The temperature of the gas phase inside the collapsing bubbles can reach as high as 5000 K [69] in water, with the heating and cooling rates ~ 10^{10} K/s [70], leading to membrane injury, nutrient and ion losses, ribosome aggregation, rupture of DNA filaments, and protein coagulation, etc. [71]. Under the extreme high-pressure and temperature conditions created by cavitation, highly reactive hydroxyl radicals (OH·) can be generated by the sonolysis of water molecules [72]. OH· can cause radical chain reactions, generating various types of reactive oxygen species. They oxidize sulfhydryl groups and double bonds in proteins, lipids, and membrane surfaces and result in irreversible damage to microorganisms [73].

In summary, the hydrodynamical and sonochemical effects induced by the ARHCR are highly destructive to *E. coli*, which is needed to be further investigated and confirmed in future.

4. Conclusion

In the present study, the pilot-scale ARHCR was applied to water disinfection. The effects of operational conditions on disinfection effectiveness were revealed and analyzed. The performance was compared with that of previous HCRs. A new possible disinfection mechanism of the ARHCR was proposed. The main findings are as follows.

- Increasing the rotational speed and decreasing the flow rate were beneficial to disinfection, while the final treatment temperature was not associated with the disinfection in batch mode.

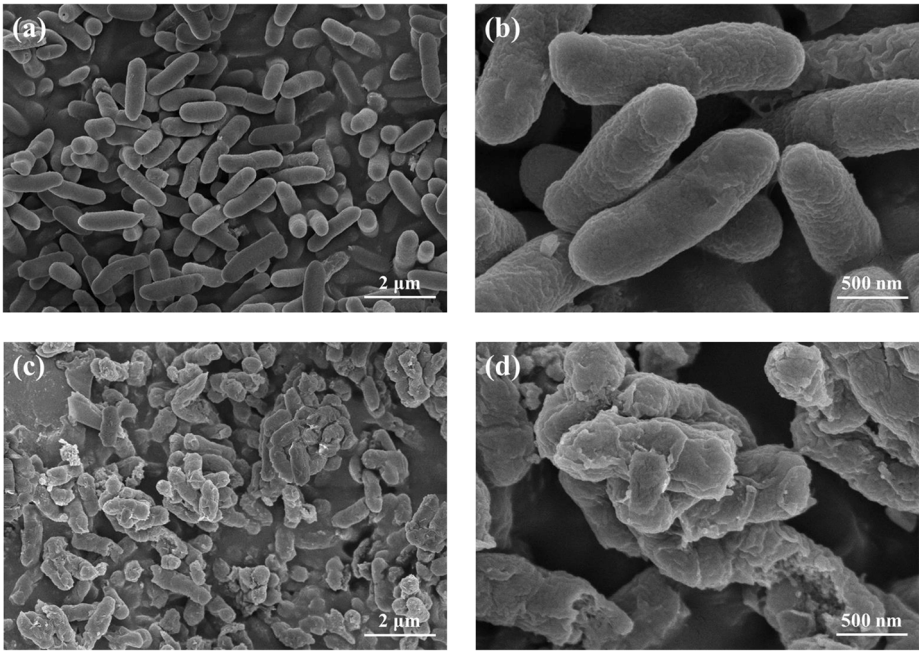

Fig. 7. Scanning electron micrographs of *E. coli* cells before ((a) 0 min (×10,000) and (b) 0 min (×40,000)) and after ((c) 10 min (×10,000) and (d) 10 min (×40,000)) the ARHCR treatment at 3800 rpm and 1.4 m^3/h.

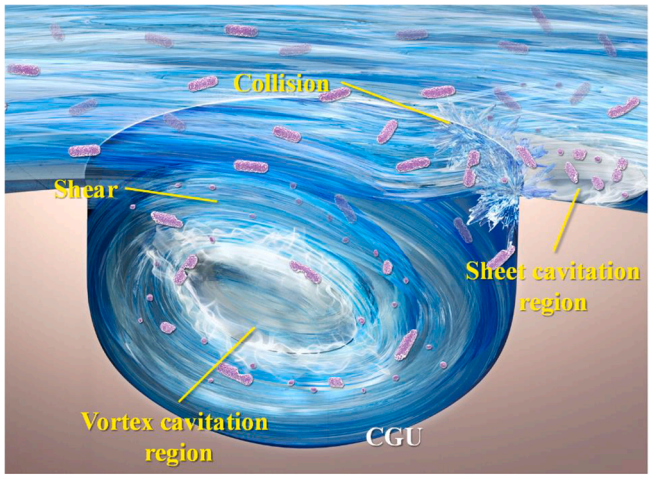

(a)

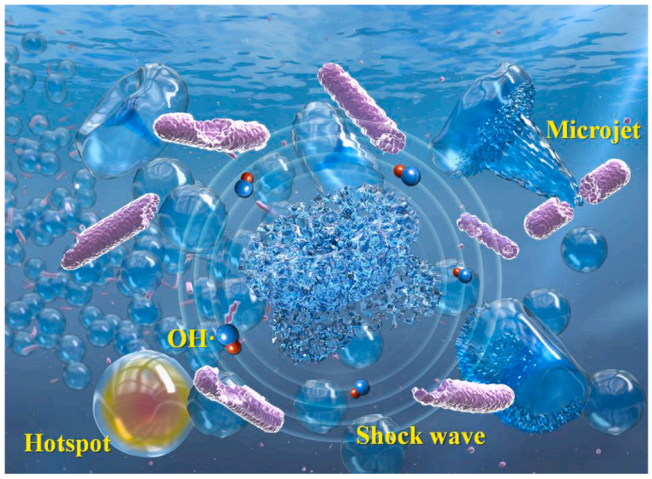

(b)

Fig. 8. Possible disinfection mechanism of the ARHCR: (a) hydrodynamical and (b) sonochemical effects.

- Thermal performance was not a universal index characterizing cavitation intensity induced by HCRs.
- A decrease in C_v contributed to the rapid increases in both the log reduction and reaction rate constant.
- 100% disinfection rate of *E. coli* can be obtained at 4200 rpm and 1.4 m^3/h in 4 min for 15 L of simulated effluent, with energy efficiency of 0.0499 kWh/L. The time and cost efficiencies of the ARHCR were considerably greater than those of previous HCRs.
- The ARHCR can cause serious cleavage and surface damages to *E. coli*.
- The possible disinfection mechanism of the ARHCR includes hydrodynamical and sonochemical effects, which cannot be obtained by conventional HCRs.

The ARHCR can be utilized as a promising alternative or complementary tool for water disinfection as well as other process intensifications. Further research on the disinfection mechanism, structural optimization, and scale up are needed in future.

CRediT authorship contribution statement

Xun Sun: Investigation, Methodology, Writing - original draft. **Zhengquan Wang:** Methodology. **Xiaoxu Xuan:** Writing - review & editing, Conceptualization. **Li Ji:** Writing - review & editing. **Xuewen Li:** Writing - review & editing. **Yang Tao:** Writing - review & editing. **Grzegorz Boczkaj:** Writing - review & editing. **Shan Zhao:** Writing - review & editing. **Joon Yong Yoon:** Writing - review & editing. **Songying Chen:** Conceptualization, Supervision.

Declaration of Competing Interest

The authors declare that they have no known competing financial interests or personal relationships that could have appeared to influence the work reported in this paper.

Acknowledgements

This work was supported by the National Natural Science Foundation of China (grant nos. 51906125, U2006221); China Postdoctoral Science Foundation (grant nos. 2020T130364, 2019M650162); Postdoctoral Innovation Project of Shandong Province (grant no. 202002006); Shandong Provincial Natural Science Foundation (grant no. ZR2020KB004); Youth Interdisciplinary Science and Innovative Research Groups of Shandong University (grant no. 2020QNQT014); Young Scholars Program of Shandong University; Fundamental Research Funds of Shandong University (grant nos. 2019HW027, 2020GN050, 2019HW041); Key Research and Development Project of Zibo City (grant no. 2020XCCG0160); Ocean Industry Leading Talent Team of Yantai's Double Hundred Plan; and National Science Centre, Poland (decision no. UMO-2017/25/B/ST8/01364).

Appendix A. Supplementary data

Supplementary data to this article can be found online at https://doi.org/10.1016/j.ultsonch.2021.105543.

References

[1] Z. Chen, X. Xu, Z. Ding, K. Wang, X. Sun, T. Lu, M. Konarova, M. Eguchi, J. G. Shapter, L. Pan, Y. Yamauchi, Ti_3C_2 MXenes-derived $NaTi_2(PO_4)_3$/MXene nanohybrid for fast and efficient hybrid capacitive deionization performance, Chem. Eng. J. 407 (2021), 127148, https://doi.org/10.1016/j.cej.2020.127148.

[2] Z. Zhuge, X. Liu, T. Chen, Y. Gong, C. Li, L. Niu, S. Xu, X. Xu, Z.A. Alothman, C. Q. Sun, J.G. Shapter, Y. Yamauchi, Highly efficient photocatalytic degradation of different hazardous contaminants by $CaIn_2S_4$-$Ti_3C_2T_x$ Schottky heterojunction: An experimental and mechanism study, Chem. Eng. J. (2020) 127838, https://doi.org/10.1016/j.cej.2020.127838.

[3] WHO, Dringking-Water. https://www.who.int/news-room/fact-sheets/detail/drinking-water, 2019 (accessed 14 June 2019).

[4] M. Zupanc, Ž. Pandur, T. Stepišnik Perdih, D. Stopar, M. Petkovšek, M. Dular, Effects of cavitation on different microorganisms: The current understanding of the mechanisms taking place behind the phenomenon. A review and proposals for further research, Ultrason. Sonochem. 57 (2019) 147–165, https://doi.org/10.1016/j.ultsonch.2019.05.009.

[5] M.A. Würtele, T. Kolbe, M. Lipsz, A. Külberg, M. Weyers, M. Kneissl, M. Jekel, Application of GaN-based ultraviolet-C light emitting diodes – UV LEDs – for water disinfection, Water Res. 45 (3) (2011) 1481–1489, https://doi.org/10.1016/j.watres.2010.11.015.

[6] B.R. Kim, J.E. Anderson, S.A. Mueller, W.A. Gaines, A.M. Kendall, Literature review—efficacy of various disinfectants against *Legionella* in water systems, Water Res. 36 (18) (2002) 4433–4444, https://doi.org/10.1016/S0043-1354(02)00188-4.

[7] A. Kraft, Electrochemical Water Disinfection: A Short Review, Platinum Met. Rev. 52 (3) (2008) 177–185, https://doi.org/10.1595/147106708X329273.

[8] O.K. Dalrymple, E. Stefanakos, M.A. Trotz, D.Y. Goswami, A review of the mechanisms and modeling of photocatalytic disinfection, Appl. Catal. B 98 (1–2) (2010) 27–38, https://doi.org/10.1016/j.apcatb.2010.05.001.

[9] N. Pichel, M. Vivar, M. Fuentes, The problem of drinking water access: A review of disinfection technologies with an emphasis on solar treatment methods, Chemosphere 218 (2019) 1014–1030, https://doi.org/10.1016/j.chemosphere.2018.11.205.

[10] L.Y. Ozer, A. Yusuf, J.M. Uratani, B. Cabal, L.A. Díaz, R. Torrecillas, J.S. Moya, J. Rodríguez, G. Palmisano, Water microbial disinfection via supported nAg/Kaolin in a fixed-bed reactor configuration, Appl. Clay Sci. 184 (2020) 105387, https://doi.org/10.1016/j.clay.2019.105387.

[11] M.B. Mane, V.M. Bhandari, K. Balapure, V.V. Ranade, A novel hybrid cavitation process for enhancing and altering rate of disinfection by use of natural oils derived from plants, Ultrason. Sonochem. 61 (2020) 104820, https://doi.org/10.1016/j.ultsonch.2019.104820.

[12] M. Dular, T. Griessler-Bulc, I. Gutierrez-Aguirre, E. Heath, T. Kosjek, A. Krivograd Klemenčič, M. Oder, M. Petkovšek, N. Rački, M. Ravnikar, A. Šarc, B. Širok,

M. Zupanc, M. Žitnik, B. Kompare, Use of hydrodynamic cavitation in (waste)water treatment, Ultrason. Sonochem. 29 (2016) 577–588, https://doi.org/10.1016/j.ultsonch.2015.10.010.
[13] T.A. Bashir, A.G. Soni, A.V. Mahulkar, A.B. Pandit, The CFD driven optimisation of a modified venturi for cavitational activity, Can. J. Chem. Eng. 89 (6) (2011) 1366–1375, https://doi.org/10.1002/cjce:v89.610.1002/cjce:20500.
[14] S. Raut-Jadhav, M.P. Badve, D.V. Pinjari, D.R. Saini, S.H. Sonawane, A.B. Pandit, Treatment of the pesticide industry effluent using hydrodynamic cavitation and its combination with process intensifying additives (H_2O_2 and ozone), Chem. Eng. J. 295 (2016) 326–335, https://doi.org/10.1016/j.cej.2016.03.019.
[15] M. Zupanc, T. Kosjek, M. Petkovšek, M. Dular, B. Kompare, B. Širok, M. Stražar, E. Heath, Shear-induced hydrodynamic cavitation as a tool for pharmaceutical micropollutants removal from urban wastewater, Ultrason. Sonochem. 21 (3) (2014) 1213–1221, https://doi.org/10.1016/j.ultsonch.2013.10.025.
[16] V.O. Abramov, A.V. Abramova, G. Cravotto, R.V. Nikonov, I.S. Fedulov, V. K. Ivanov, Flow-mode water treatment under simultaneous hydrodynamic cavitation and plasma, Ultrason. Sonochem. 70 (2021) 105323, https://doi.org/10.1016/j.ultsonch.2020.105323.
[17] T.J. Mason, E. Joyce, S.S. Phull, J.P. Lorimer, Potential uses of ultrasound in the biological decontamination of water, Ultrason. Sonochem. 10 (6) (2003) 319–323, https://doi.org/10.1016/S1350-4177(03)00102-0.
[18] M. Gągol, A. Przyjazny, G. Boczkaj, Wastewater treatment by means of advanced oxidation processes based on cavitation – A review, Chem. Eng. J. 338 (2018) 599–627, https://doi.org/10.1016/j.cej.2018.01.049.
[19] K. Fedorov, X. Sun, G. Boczkaj, Combination of hydrodynamic cavitation and SR-AOPs for simultaneous degradation of BTEX in water, Chem. Eng. J. (2020) 128081, https://doi.org/10.1016/j.cej.2020.128081.
[20] X. Sun, S. Chen, J. Liu, S. Zhao, J.Y. Yoon, Hydrodynamic Cavitation: A Promising Technology for Industrial-Scale Synthesis of Nanomaterials, Front. Chem. 8 (2020) 259, https://doi.org/10.3389/fchem.2020.00259.
[21] A. Šarc, J. Kosel, D. Stopar, M. Oder, M. Dular, Removal of bacteria *Legionella pneumophila*, *Escherichia coli*, and *Bacillus subtilis* by (super)cavitation, Ultrason. Sonochem. 42 (2018) 228–236, https://doi.org/10.1016/j.ultsonch.2017.11.004.
[22] A. Kovačič, D. Škufca, M. Zupanc, J. Gostiša, B. Bizjan, N. Krištofelc, M.S. Dolenc, E. Heath, The removal of bisphenols and other contaminants of emerging concern by hydrodynamic cavitation: From lab-scale to pilot-scale, Sci. Total Environ. 743 (2020) 140724, https://doi.org/10.1016/j.scitotenv.2020.140724.
[23] S.B. Gregersen, L. Wiking, D.J. Metto, K. Bertelsen, B. Pedersen, K.R. Poulsen, U. Andersen, M. Hammershøj, Hydrodynamic cavitation of raw milk: Effects on microbial inactivation, physical and functional properties, Int. Dairy J. 109 (2020) 104790, https://doi.org/10.1016/j.idairyj.2020.104790.
[24] M.P. Badve, P.R. Gogate, A.B. Pandit, L. Csoka, Hydrodynamic cavitation as a novel approach for delignification of wheat straw for paper manufacturing, Ultrason. Sonochem. 21 (1) (2014) 162–168, https://doi.org/10.1016/j.ultsonch.2013.07.006.
[25] H. Kim, X. Sun, B. Koo, J.Y. Yoon, Experimental Investigation of Sludge Treatment Using a Rotor-Stator Type Hydrodynamic Cavitation Reactor and an Ultrasonic Bath, Processes 7 (11) (2019) 790, https://doi.org/10.3390/pr7110790.
[26] J. Kosel, A. Šinkovec, M. Dular, A novel rotation generator of hydrodynamic cavitation for the fibrillation of long conifer fibers in paper production, Ultrason. Sonochem. 59 (2019) 104721, https://doi.org/10.1016/j.ultsonch.2019.104721.
[27] P. Chipurici, A. Vlaicu, I. Calinescu, M. Vinatoru, M. Vasilescu, N.D. Ignat, T. J. Mason, Ultrasonic, hydrodynamic and microwave biodiesel synthesis – A comparative study for continuous process, Ultrason. Sonochem. 57 (2019) 38–47, https://doi.org/10.1016/j.ultsonch.2019.05.011.
[28] B. Maršálek, Š. Zezulka, E. Maršálková, F. Pochylý, P. Rudolf, Synergistic effects of trace concentrations of hydrogen peroxide used in a novel hydrodynamic cavitation device allows for selective removal of cyanobacteria, Chem. Eng. J. 382 (2020) 122383, https://doi.org/10.1016/j.cej.2019.122383.
[29] P.J. Milly, R.T. Toledo, W.L. Kerr, D. Armstead, Hydrodynamic Cavitation: Characterization of a Novel Design with Energy Considerations for the Inactivation of *Saccharomyces cerevisiae* in Apple Juice, J. Food Sci. 73 (2008) M298–M303, https://doi.org/10.1111/j.1750-3841.2008.00827.x.
[30] P.J. Milly, R.T. Toledo, M.A. Harrison, D. Armstead, Inactivation of Food Spoilage Microorganisms by Hydrodynamic Cavitation to Achieve Pasteurization and Sterilization of Fluid Foods, J. Food Sci. 72 (9) (2007) M414–M422, https://doi.org/10.1111/jfds.2007.72.issue-910.1111/j.1750-3841.2007.00543.x.
[31] L.M. Cerecedo, C. Dopazo, R. Gomez-Lus, Water disinfection by hydrodynamic cavitation in a rotor-stator device, Ultrason. Sonochem. 48 (2018) 71–78, https://doi.org/10.1016/j.ultsonch.2018.05.015.
[32] X. Sun, J.J. Park, H.S. Kim, S.H. Lee, S.J. Seong, A.S. Om, J.Y. Yoon, Experimental investigation of the thermal and disinfection performances of a novel hydrodynamic cavitation reactor, Ultrason. Sonochem. 49 (2018) 13–23, https://doi.org/10.1016/j.ultsonch.2018.02.039.
[33] X. Sun, X. Jia, J. Liu, G. Wang, S. Zhao, L. Ji, J.Y. Yoon, S. Chen, Investigation on the Characteristics of an Advanced Rotational Hydrodynamic Cavitation Reactor for Water Treatment, Sep. Purif. Technol. 251 (2020) 117252, https://doi.org/10.1016/j.seppur.2020.117252.
[34] X. Sun, X. Xuan, Y. Song, X. Jia, L. Ji, S. Zhao, J.Y. Yoon, S. Chen, J. Liu, G. Wang, Experimental and numerical studies on the cavitation in an advanced rotational hydrodynamic cavitation reactor for water treatment, Ultrason. Sonochem. 70 (2021) 105311, https://doi.org/10.1016/j.ultsonch.2020.105311.
[35] X. Sun, X. Xuan, L. Ji, S. Chen, J. Liu, S. Zhao, S. Park, J.Y. Yoon, A.S. Om, A novel continuous hydrodynamic cavitation technology for the inactivation of pathogens in milk, Ultrason. Sonochem. 71 (2021) 105382, https://doi.org/10.1016/j.ultsonch.2020.105382.
[36] X. Sun, C.H. Kang, J.J. Park, H.S. Kim, A.S. Om, J.Y. Yoon, An experimental study on the thermal performance of a novel hydrodynamic cavitation reactor, Exp. Therm Fluid Sci. 99 (2018) 200–210, https://doi.org/10.1016/j.expthermflusci.2018.02.034.
[37] M. Badve, P. Gogate, A. Pandit, L. Csoka, Hydrodynamic cavitation as a novel approach for wastewater treatment in wood finishing industry, Sep. Purif. Technol. 106 (2013) 15–21, https://doi.org/10.1016/j.seppur.2012.12.029.
[38] J. Kosel, M. Šuštaršič, M. Petkovšek, M. Zupanc, M. Sežun, M. Dular, Application of (super)cavitation for the recycling of process waters in paper producing industry, Ultrason. Sonochem. 64 (2020) 105002, https://doi.org/10.1016/j.ultsonch.2020.105002.
[39] M. Petkovšek, M. Mlakar, M. Levstek, M. Stražar, B. Širok, M. Dular, A novel rotation generator of hydrodynamic cavitation for waste-activated sludge disintegration, Ultrason. Sonochem. 26 (2015) 408–414, https://doi.org/10.1016/j.ultsonch.2015.01.006.
[40] H. Kim, B. Koo, X. Sun, J.Y. Yoon, Investigation of sludge disintegration using rotor-stator type hydrodynamic cavitation reactor, Sep. Purif. Technol. 240 (2020) 116636, https://doi.org/10.1016/j.seppur.2020.116636.
[41] L. Naderloo, Energy ratio of produced biodiesel in hydrodynamic cavitation reactor equipped with LabVIEW controller and artificial intelligence, Energy Reports 6 (2020) 1456–1467, https://doi.org/10.1016/j.egyr.2020.05.029.
[42] G. Zhang, Y.F. Zhang, Q. Liu, Y. Li, Z. Lin, Experimental study on the two-phase flow of gas-particles through a model brake valve, Powder Technol. 367 (2020) 172–182, https://doi.org/10.1016/j.powtec.2020.03.047.
[43] J.P. Tullis, Hydraulics of pipelines: Pumps, valves, cavitation, transients, John Wiley & Sons, Hoboken, 1989.
[44] E. Burzio, F. Bersani, G.C.A. Caridi, R. Vesipa, L. Ridolfi, C. Manes, Water disinfection by orifice-induced hydrodynamic cavitation, Ultrason. Sonochem. 60 (2020) 104740, https://doi.org/10.1016/j.ultsonch.2019.104740.
[45] M. Wan, Y. Feng, G.t. Haar, Cavitation in Biomedicine: Principles and Techniques, Springer, Netherlands, Brulin, 2015.
[46] G. Mancuso, M. Langone, G. Andreottola, L. Bruni, Effects of hydrodynamic cavitation, low-level thermal and low-level alkaline pre-treatments on sludge solubilisation, Ultrason. Sonochem. 59 (2019) 104750, https://doi.org/10.1016/j.ultsonch.2019.104750.
[47] G. Li, L. Yi, J. Wang, Y. Song, Hydrodynamic cavitation degradation of Rhodamine B assisted by Fe^{3+}-doped TiO_2: Mechanisms, geometric and operation parameters, Ultrason. Sonochem. 60 (2020) 104806, https://doi.org/10.1016/j.ultsonch.2019.104806.
[48] S. Joshi, P.R. Gogate, P.F. Moreira, R. Giudici, Intensification of biodiesel production from soybean oil and waste cooking oil in the presence of heterogeneous catalyst using high speed homogenizer, Ultrason. Sonochem. 39 (2017) 645–653, https://doi.org/10.1016/j.ultsonch.2017.05.029.
[49] Z. Wu, H. Shen, B. Ondruschka, Y. Zhang, W. Wang, D.H. Bremner, Removal of blue-green algae using the hybrid method of hydrodynamic cavitation and ozonation, J. Hazard. Mater. 235–236 (2012) 152–158, https://doi.org/10.1016/j.jhazmat.2012.07.034.
[50] R. Chand, D.H. Bremner, K.C. Namkung, P.J. Collier, P.R. Gogate, Water disinfection using the novel approach of ozone and a liquid whistle reactor, Biochem. Eng. J. 35 (3) (2007) 357–364, https://doi.org/10.1016/j.bej.2007.01.032.
[51] S. Arrojo, Y. Benito, A. Martínez Tarifa, A parametrical study of disinfection with hydrodynamic cavitation, Ultrason. Sonochem. 15 (5) (2008) 903–908, https://doi.org/10.1016/j.ultsonch.2007.11.001.
[52] L. Mezule, S. Tsyfansky, V. Yakushevich, T. Juhna, A simple technique for water disinfection with hydrodynamic cavitation: Effect on survival of *Escherichia coli*, Desalination 248 (1–3) (2009) 152–159, https://doi.org/10.1016/j.desal.2008.05.051.
[53] G. Loraine, G. Chahine, C.-T. Hsiao, J.-K. Choi, P. Aley, Disinfection of gram-negative and gram-positive bacteria using DynaJets® hydrodynamic cavitating jets, Ultrason. Sonochem. 19 (3) (2012) 710–717, https://doi.org/10.1016/j.ultsonch.2011.10.011.
[54] José.G. Dalfré Filho, M.P. Assis, A.Inés.B. Genovez, Bacterial inactivation in artificially and naturally contaminated water using a cavitating jet apparatus, J. Hydro-environ. Res. 9 (2) (2015) 259–267, https://doi.org/10.1016/j.jher.2015.03.001.
[55] P. Jain, V.M. Bhandari, K. Balapure, J. Jena, V.V. Ranade, D.J. Killedar, Hydrodynamic cavitation using vortex diode: An efficient approach for elimination of pathogenic bacteria from water, J. Environ. Manage. 242 (2019) 210–219, https://doi.org/10.1016/j.jenvman.2019.04.057.
[56] M.B. Mane, V.M. Bhandari, K. Balapure, V.V. Ranade, Destroying antimicrobial resistant bacteria (AMR) and difficult, opportunistic pathogen using cavitation and natural oils/plant extract, Ultrason. Sonochem. 69 (2020) 105272, https://doi.org/10.1016/j.ultsonch.2020.105272.
[57] X. Sun, J. Liu, L. Ji, G. Wang, S. Zhao, J.Y. Yoon, S. Chen, A review on hydrodynamic cavitation disinfection: The current state of knowledge, Sci. Total Environ. 737 (2020) 139606, https://doi.org/10.1016/j.scitotenv.2020.139606.
[58] S. Zhang, P. Zhang, G. Zhang, J. Fan, Y. Zhang, Enhancement of anaerobic sludge digestion by high-pressure homogenization, Bioresour. Technol. 118 (2012) 496–501, https://doi.org/10.1016/j.biortech.2012.05.089.
[59] I. Lee, J.-I. Han, The effects of waste-activated sludge pretreatment using hydrodynamic cavitation for methane production, Ultrason. Sonochem. 20 (6) (2013) 1450–1455, https://doi.org/10.1016/j.ultsonch.2013.03.006.
[60] K.-W. Jung, M.-J. Hwang, Y.-M. Yun, M.-J. Cha, K.-H. Ahn, Development of a novel electric field-assisted modified hydrodynamic cavitation system for disintegration

of waste activated sludge, Ultrason. Sonochem. 21 (5) (2014) 1635–1640, https://doi.org/10.1016/j.ultsonch.2014.04.008.
[61] G. Mancuso, M. Langone, G. Andreottola, A swirling jet-induced cavitation to increase activated sludge solubilisation and aerobic sludge biodegradability, Ultrason. Sonochem. 35 (2017) 489–501, https://doi.org/10.1016/j.ultsonch.2016.11.006.
[62] M. Nabi, G. Zhang, P. Zhang, X. Tao, S. Wang, J. Ye, Q. Zhang, M. Zubair, S. Bao, Y. Wu, Contribution of solid and liquid fractions of sewage sludge pretreated by high pressure homogenization to biogas production, Bioresour. Technol. 286 (2019) 121378, https://doi.org/10.1016/j.biortech.2019.121378.
[63] L. Xie, A. Terada, M. Hosomi, Disentangling the multiple effects of a novel high pressure jet device upon bacterial cell disruption, Chem. Eng. J. 323 (2017) 105–113, https://doi.org/10.1016/j.cej.2017.04.067.
[64] J. Holzfuss, M. Rüggeberg, A. Billo, Shock Wave Emissions of a Sonoluminescing Bubble, Phys. Rev. Lett. 81 (24) (1998) 5434–5437, https://doi.org/10.1103/PhysRevLett.81.5434.
[65] A. Vogel, S. Busch, U. Parlitz, Shock wave emission and cavitation bubble generation by picosecond and nanosecond optical breakdown in water, J. Acoust. Soc. Am. 100 (1) (1996) 148–165, https://doi.org/10.1121/1.415878.
[66] A. Vogel, W. Lauterborn, R. Timm, Optical and acoustic investigations of the dynamics of laser-produced cavitation bubbles near a solid boundary, J. Fluid Mech. 206 (1989) 299–338, https://doi.org/10.1017/S0022112089002314.
[67] A. Philipp, W. Lauterborn, Cavitation erosion by single laser-produced bubbles, J. Fluid Mech. 361 (1998) 75–116, https://doi.org/10.1017/S0022112098008738.
[68] R. Dijkink, C.-D. Ohl, Measurement of cavitation induced wall shear stress, Appl. Phys. Lett. 93 (25) (2008) 254107, https://doi.org/10.1063/1.3046735.
[69] K.S. Suslick, D.A. Hammerton, R.E. Cline, Sonochemical hot spot, J. Am. Chem. Soc. 108 (18) (1986) 5641–5642, https://doi.org/10.1021/ja00278a055.
[70] K.S. Suslick, Sonochemistry, Science 247 (4949) (1990) 1439–1445, https://doi.org/10.1126/science:247.4949.1439.
[71] P. Mañas, R. Pagán, Microbial inactivation by new technologies of food preservation, J. Appl. Microbiol. 98 (2005) 1387–1399, https://doi.org/10.1111/j.1365-2672.2005.02561.x.
[72] G. Boczkaj, A. Fernandes, Wastewater treatment by means of advanced oxidation processes at basic pH conditions: A review, Chem. Eng. J. 320 (2017) 608–633, https://doi.org/10.1016/j.cej.2017.03.084.
[73] Y. Kobayashi, M. Hayashi, F. Yoshino, M. Tamura, A. Yoshida, H. Ibi, M.-C.-il. Lee, K. Ochiai, B. Ogiso, Bactericidal effect of hydroxyl radicals generated from a low concentration hydrogen peroxide with ultrasound in endodontic treatment, J. Clin. Biochem. Nutr. 54 (3) (2014) 161–165, https://doi.org/10.3164/jcbn.13-86.